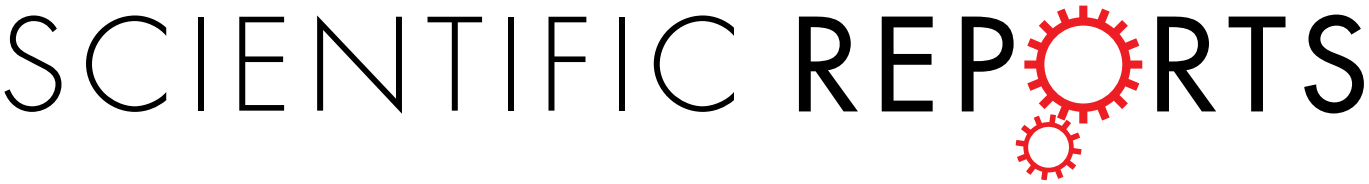

OPEN

Berry phase theory of planar Hall effect in topological insulators

S. Nandy[1], A. Taraphder[1,2,3] & Sumanta Tewari[1,4]

Received: 25 June 2018
Accepted: 26 September 2018
Published online: 08 October 2018

The appearance of negative longitudinal magnetoresistance (LMR) in topological semimetals such as Weyl and Dirac semimetals is understood as an effect of chiral anomaly, whereas such an anomaly is not well-defined in topological insulators. Nevertheless, it has been shown recently in both theory and experiments that nontrivial Berry phase effects can give rise to negative LMR in topological insulators even in the absence of chiral anomaly. In this paper, we present a quasi-classical theory of another intriguing phenomenon in topological insulators – also ascribed to chiral anomaly in Weyl and Dirac semimetals– the so-called planar Hall effect (PHE). PHE implies the appearance of a transverse voltage in the plane of applied non-parallel electric and magnetic fields, in a configuration in which the conventional Hall effect vanishes. Starting from Boltzmann transport equations we derive the expressions for PHE and LMR in topological insulators in the bulk conduction limit, and show the important role played by orbital magnetic moment. Our theoretical results for magnetoconductance with non-parallel electric and magnetic fields predict detailed experimental signatures in topological insulators – specifically of planar Hall effect – that can be observed in experiments.

Three-dimensional (3D) topological insulators (TI) as a new class of quantum matter have recently drawn much attention in condensed matter physics and materials science[1,2]. In TIs, a finite energy gap is present in the bulk, which is crossed by two gapless surface state branches with nontrivial spin textures protected from backscattering by time reversal symmetry. In these systems, owing to strong spin-orbit coupling, electron spins in the surface state branches are aligned perpendicular to their momenta contributing an overall Berry phase of π to the fermion wave functions. In addition to the fundamental scientific interest, TIs evince a wide variety of intriguing transport properties which make them potential candidates for technological applications. For instance, the topological protection of the surface states and the nontrivial spin textures can be of interest for spintronic and quantum computation applications[1].

Several transport studies on TIs have revealed various anomalous quantum phenomena associated with the topological surface states, such as the Aharonov-Bohm oscillations in Bi_2Se_3 nanoribbons[3], the weak anti-localization in Bi_2Se_3 and Bi_2Te_3 thin films[4–6], and the two-dimensional SdH oscillations in Bi_2Te_3[7]. Very recently, another intriguing phenomenon, negative longitudinal magnetoresistance (LMR) (and conversely, positive longitudinal magnetoconductivity (LMC)) in the presence of parallel electric and magnetic fields, has been discovered from the bulk conduction contribution in 3D topological insulators[8–12]. The observation of this effect in TIs is quite puzzling because the negative LMR in topological semimetals such as Weyl semimetals is widely believed to be due to non-conservation of separate electron numbers of opposite chirality for relativistic massless fermions, an effect known as the chiral or Adler-Bell-Jackiw anomaly[13–23]. Several experimental groups have successfully observed the chiral anomaly induced negative LMR in Dirac and Weyl materials[24–29]. But this picture of chiral anomaly induced negative longitudinal magnetoresistance does not work in topological insulators because chiral anomaly itself is not well defined in these systems. In recent theoretical work, the negative longitudinal magnetoresistance in topological insulators has been discussed in terms of non-trivial Berry phase effects in the absence of chiral anomaly[30].

It was suggested earlier that a positive LMC is not the only effect of chiral anomaly in a topological Weyl semimetal[31,32]. A second effect of chiral anomaly is the so-called planar Hall effect, i.e., appearance of an in-plane transverse voltage when the co-planar electric and magnetic fields are not perfectly aligned to each other, precisely in a configuration in which the Lorentz force induced conventional Hall effect vanishes. The planar Hall

[1]Department of Physics, Indian Institute of Technology Kharagpur, Kharagpur, 721302, India. [2]Centre for Theoretical Studies and Centre for Nanoscience and Nanotechnology, Indian Institute of Technology Kharagpur, Kharagpur, 721302, India. [3]School of Basic Sciences, Indian Institute of Technology Mandi, Kamand, 175005, India. [4]Department of Physics and Astronomy, Clemson University, Clemson, SC, 29634, USA. Correspondence and requests for materials should be addressed to S.N. (email: snehasish@phy.iitkgp.ernet.in)

conductivity (PHC) is defined as the transverse conductivity measured along $\hat{y}$, in a direction perpendicular to the applied electric field and current along $\hat{x}$, in the presence of a magnetic field in the $x-y$ plane making an angle θ with the x axis. This effect is known to occur in ferromagnetic systems[33–37] where its origin is non-trivial spin topology. Interestingly, it has also been observed recently in the surface states of a topological insulator where it has been linked to magnetic field induced anisotropic lifting of the protection of the surface states from backscattering[38]. The main objective of our work is to suggest the existence of planar Hall effect, from the bulk states of 3D topological insulators, in systems exhibiting negative longitudinal magnetoresistance[8–12]. We use a semi-classical Boltzmann transport theory incorporating topological Berry phase effects to show this. In a complete theory we also derive the associated expressions for longitudinal magnetoconductivity in topological insulators in the bulk conduction limit as discussed previously[30]. We predict specific magnitudes and direction dependence of PHC and LMC on the applied fields that can be tested in experiments.

In this paper we have chosen Bi_2Se_3 as a reference 3D strong topological insulator and study the PHC and LMC expected from its bulk states. This material has been clearly identified as a 3D strong topological insulator with a bulk band gap of 0.3 eV, with a single spin-helical Dirac cone on each surface, which has been confirmed in angle-resolved photoemission spectroscopy measurement[39]. Our work on planar Hall effect in this system, together with positive longitudinal magnetoconductance[30], completes the quasi-classical description of Berry curvature induced anomalous magneto-transport phenomena in three dimensional topological insulators in the bulk conduction limit.

The rest of the paper is organized as follows. First, we introduce the effective Hamiltonian for the bulk states of a 3D strong topological insulator Bi_2Se_3. Next we derive the analytical expressions of LMC and PHC using semiclassical Boltzmann transport equations. Then we show our numerical results on LMC and PHC establishing the anomalous features in the transport properties. We also make comparison of our results with existing experimental data. Finally we discuss the experimental aspects of the phenomena observed in our study and end with a brief conclusion.

Results

Model Hamiltonian. The low-energy long-wavelength properties of a 3D topological insulator in the presence of time reversal and space inversion symmetries can be described by the effective $\mathbf{k}\cdot\mathbf{p}$ Hamiltonian. In the basis of $(\psi_{v\uparrow}, \psi_{v\downarrow}, \psi_{c\uparrow}, \psi_{c\downarrow})$, where v and c denotes the valence and conduction band, the effective Hamiltonian can be written as

$$\mathcal{H}_0(\mathbf{k}) = \varepsilon_{\mathbf{k}} I_{4\times 4} + M_{\mathbf{k}}\tau_z\sigma_0 + V_{\parallel}(\tau_x\sigma_y k_x - \tau_x\sigma_x k_y) - V_n\tau_y\sigma_0 k_z \tag{1}$$

where $\varepsilon_{\mathbf{k}} = C_0 + C_{\parallel}\mathbf{k}_{\parallel}^2 + C_z k_z^2$, $M_{\mathbf{k}} = M_0 + M_{\parallel}\mathbf{k}_{\parallel}^2 + M_z k_z^2$, and $k_{\parallel}^2 = k_x^2 + k_y^2$ with C_i, M_i, and V_i as model parameters. σ, τ are the Pauli matrices in spin and orbital space, respectively. In the present work we have taken $C_0 = 0.048$ eV, $C_{\parallel} = 13.9$ eV-Å^2, $C_z = 1.409$ eV-Å^2, $M_0 = -0.169$ eV, $M_{\parallel} = 29.36$ eV-Å^2, $M_z = 3.351$ eV-Å^2, $V_n = 1.853$ eV-Å, and $V_{\parallel} = 2.512$ eV-Å to represent the Bi_2Se_3 topological insulator as suggested by the ab-initio bandstructure calculations[40,41]. The Hamiltonian described by the Eq. (1) includes uniaxial anisotropy along the z-direction and k-dependent mass terms. $M_0 M_{\parallel} < 0$ and $M_0 M_z < 0$ implies that this model belongs to a 3D strong topological insulator[42]. The 3D dispersion of the four bulk bands near the Γ point, two degenerate conduction bands and valencebands each, is depicted in Fig. 1(a). To compute the longitudinal conductivity and planar Hall conductivity in the bulk conduction limit we have assumed that the Fermi level crosses the conduction bands.

In addition to the band energy, the Berry curvature $\Omega(\mathbf{k})$ of the Bloch bands is required for a complete description of the electron dynamics in topological systems. The general form of the Berry curvature can be obtained via symmetry analysis. Under time reversal symmetry, the Berry curvature satisfies $\Omega(-\mathbf{k}) = -\Omega(\mathbf{k})$. On the other hand, if the system has spatial inversion symmetry, then $\Omega(-\mathbf{k}) = \Omega(\mathbf{k})$. Therefore, for 3D topological insualtors like Bi_2Se_3 with simultaneous time reversal and spatial inversion symmetries, the Berry curvature vanishes identically throughout the Brillouin zone for both bulk conduction and surface bands[43]. However, in the presence of a magnetic field, the Zeeman splitting breaks the time reversal symmetry and generates non-trivial Berry curvature for these bands. Therefore, for discussing magneto-transport phenomena, which by defination are in the presence of magnetic field, the effect due to non-zero Berry curvature of the bulk band should be important for the electron dynamics.

To study the Berry curvature-induced magneto-transport phenomena, in the presence of an in-plane magnetic field, we add the Zeeman magnetic term $\mathcal{H}_z$ to Eq. (1), where

$$\mathcal{H}_z = \frac{\mu_B}{2}\begin{pmatrix} 0 & g_{pv}B_- & 0 & 0 \\ g_{pv}B_+ & 0 & 0 & 0 \\ 0 & 0 & 0 & g_{pc}B_- \\ 0 & 0 & g_{pc}B_+ & 0 \end{pmatrix}. \tag{2}$$

Here μ_B is Bohr magneton and g_{pv}, g_{pc} are the Landé g factors for valence and conduction bands in the $x-y$ plane respectively. The 2D dispersions of the valence and conduction bands of the topological insulator along k_x, k_y, and k_z in the presence of an in-plane magnetic field of strength 5 T applied along x axis are shown in Fig. 1(b–d) respectively. It is clear from the figure that the dispersions of the four bands along k_x and k_y are identical. The Zeeman splitting of conduction bands is maximum (~28 meV) at the Γ point.

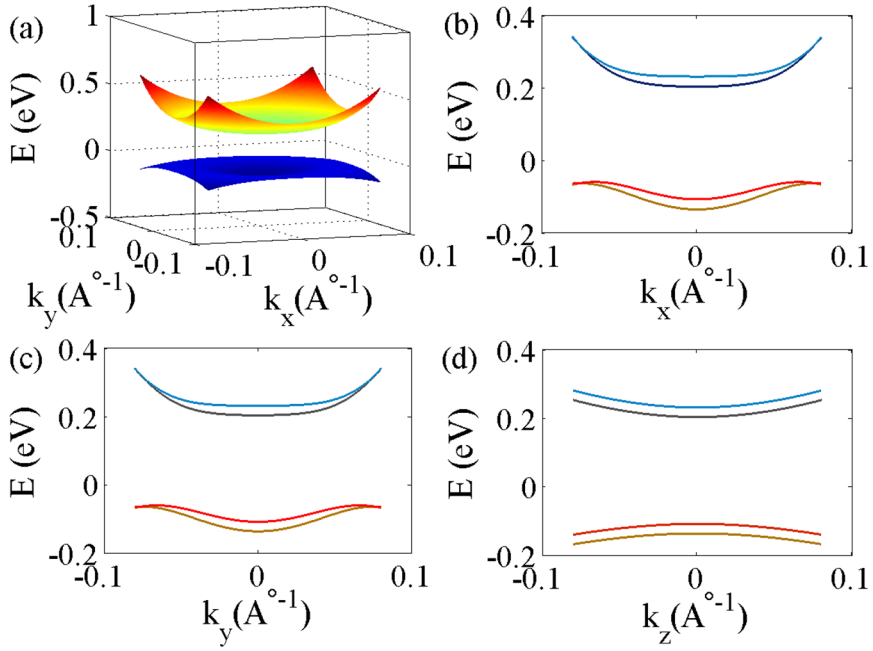

Figure 1. (**a**) 3D band dispersion of the four bands (k_z is suppressed) of 3D topological insulator (Bi_2Se_3) near Γ point obtained by diagonalizing Hamiltonian described in Eq. (1). The doubly degenerate valence bands are separated from the doubly degenerate conduction bands by an energy equal to 0.3 eV. (**b**–**d**) depict the 2D band dispersions of the same four bands as mentioned above along k_x, k_y, and k_z axis respectively in the presence of a Zeeman field of strength 5 T applied along the x direction. The Landé g-factors used here are $g_{pv} = g_{pc} = 20$[60].

Boltzmann Equation Approach For Planar Hall effect. In this section, we derive the semiclassical formulae for the planar Hall conductivity and longitudinal electrical conductivity (LEC) in the low field regime starting from the quasi-classical Boltzmann transport equation. For completeness we include the effects of the orbital magnetic moment **m**, which is the angular momentum of the semi-classical wave packet and also of geometrical origin, modifying the expressions for LEC and PHC significantly. The complete theory produces the magnetic field and direction dependence of longitudinal magnetoconductivity and planar Hall conductivity in topological insulators that can be verified in experiments.

In the presence of an electric field (**E**) and temperature gradiant (∇**T**), the charge current (**J**) and the thermal current (**Q**) flowing through the system can be described by the linear response equations,

$$\begin{pmatrix} \mathbf{J} \\ \mathbf{Q} \end{pmatrix} = \begin{pmatrix} \hat{\sigma} & \hat{\alpha} \\ \hat{\bar{\alpha}} & \hat{l} \end{pmatrix} \begin{pmatrix} \mathbf{E} \\ -\nabla \mathbf{T} \end{pmatrix} \tag{3}$$

where $\hat{\sigma}$, $\hat{\alpha}$, and $\hat{l}$ are different conductivity tensors. The tensors $\hat{\bar{\alpha}}$ and $\hat{\alpha}$ are related to each other by Onsager's relation $\hat{\bar{\alpha}} = T\hat{\alpha}$. In the linear response theory, we can write J and Q as

$$J_a = \sigma_{ab} E_b + \alpha_{ab}(-\nabla_b T) \tag{4}$$

$$Q_a = T\alpha_{ab} E_b + l_{ab}(-\nabla_b T) \tag{5}$$

The phenomenological Boltzmann transport equation in the presence of impurity scattering can be written as[44]

$$(\partial_t + \dot{\mathbf{r}} \cdot \nabla_{\mathbf{r}} + \dot{\mathbf{k}} \cdot \nabla_{\mathbf{k}}) f_{\mathbf{k},\mathbf{r},t} = C\{f_{\mathbf{k},\mathbf{r},t}\} \tag{6}$$

where on the right side $C\{f_{\mathbf{k},\mathbf{r},t}\}$ is the collision integral which incorporates electron correlations and impurity scattering effects and $f_{\mathbf{k},\mathbf{r},t}$ is the electron distribution function. Using relaxation time approximation, the collision integral takes the form $C\{f_{\mathbf{k}}\} = \frac{f_{eq} - f_k}{\tau(\mathbf{k})}$, where $\tau(\mathbf{k})$ is the relaxation time and f_{eq} is the equilibrium Fermi-Dirac distribution function in the absence of any external fields. In this paper we have ignored momentum dependence of τ and assume the parameter to be a constant in the semiclassical limit for simplifying the calculation[45]. Dropping the **r** dependence of $f_{\mathbf{k},\mathbf{r},t}$, valid for spatially uniform fields, and assuming steady state the Boltzmann equation described by Eq. (6) takes the following form

$$\dot{\mathbf{r}} \cdot \nabla_{\mathbf{r}} f_k + \dot{\mathbf{k}} \cdot \nabla_{\mathbf{k}} f_k = -\frac{\delta f}{\tau(\mathbf{k})} \tag{7}$$

In the presence of electric field and magnetic field, transport properties get substantially modified due to presence of non-trivial Berry curvature which acts as a fictitious magnetic field in the momentum space[43]. The Berry curvature of the n^{th} band for a Bloch Hamiltonian $H(\boldsymbol{k})$, defined as the Berry phase per unit area in the $\mathbf{k}$ space, is given by $\Omega^n_{\mathbf{k}} = \nabla_{\mathbf{k}} \times \langle u^n_{\mathbf{k}} | i\nabla_{\mathbf{k}} | u^n_{\mathbf{k}} \rangle$.

The wave packet of a Bloch electron also carries an orbital magnetic moment in addition to its spin moment due to the self rotation around its center of mass. The orbital magnetic moment associated with n^{th} Bloch band can be defined as[46]

$$m^n_{\mathbf{k}} = -\frac{e}{2\hbar} Im[\langle \nabla_{\mathbf{k}} u^n_{\mathbf{k}}| \times (H(\mathbf{k}) - \varepsilon_{0,\mathbf{k}}) | \nabla_{\mathbf{k}} u^n_{\mathbf{k}} \rangle] \tag{8}$$

It is clear from the above equation that the orbital magnetic moment does not depend on the actual shape and size of the wave packet but only depends on the Bloch functions. The orbital moment has exactly the same symmetry properties as the Berry curvature, namely, $m(-\mathbf{k}) = -m(\mathbf{k})$ and $m(-\mathbf{k}) = m(\mathbf{k})$ under time reversal and inversion symmetries, respectively. Therefore $m(\mathbf{k})$ vanishes in the simultaneous presence of both these symmetries. In the present case, the orbital moment is non-zero because of broken time reversal symmetry due to the in-plane magnetic field.

As the orbital moment couples to the magnetic field ($\mathbf{B}$) through a Zeeman-like term $-\mathbf{m}(\mathbf{k}) \cdot \mathbf{B}$, the unperturbed band energy $\varepsilon_{0,\mathbf{k}}$ is modified as $\varepsilon_{\mathbf{k}} = \varepsilon_{0,\mathbf{k}} - \mathbf{m}(\mathbf{k}) \cdot \mathbf{B}$. In the presence of $m(\mathbf{k})$ the group velocity of Bloch electrons is also modified as $\tilde{\mathbf{v}}_{\mathbf{k}} = \mathbf{v}_{\mathbf{k}} - \frac{1}{\hbar}\nabla(\mathbf{m} \cdot \mathbf{B})$. Incorporating the effects due to Berry curvature and orbital magnetic moment, the semi-classical equation of motion for an electron takes the following form[46]

$$\dot{\mathbf{r}} = \frac{1}{\hbar}\nabla\varepsilon_{\mathbf{k}} - \dot{\mathbf{k}} \times \Omega(\mathbf{k}) \tag{9}$$

$$\hbar\dot{\mathbf{k}} = -e\mathbf{E} - e\dot{\mathbf{r}} \times \mathbf{B} \tag{10}$$

where the second term of the Eq. (9) implies the anomalous velocity originating from the non-trivial Berry curvature. The coupled equations for $\dot{\mathbf{r}}$ and $\dot{\mathbf{k}}$ described in Eq. (9) and Eq. (10) can be solved together to obtain[47]

$$\dot{\mathbf{r}} = D(\mathbf{B}, \Omega_{\mathbf{k}})[\tilde{\mathbf{v}}_{\mathbf{k}} + \frac{e}{\hbar}(\mathbf{E} \times \Omega(\mathbf{k})) + \frac{e}{\hbar}(\tilde{\mathbf{v}}_{\mathbf{k}} \cdot \Omega(\mathbf{k}))\mathbf{B}] \tag{11}$$

$$\hbar\dot{\mathbf{k}} = -D(\mathbf{B}, \Omega_{\mathbf{k}})[e\mathbf{E} + \frac{e}{\hbar}(\tilde{\mathbf{v}}_{\mathbf{k}} \times \mathbf{B}) + \frac{e^2}{\hbar}(\mathbf{E} \cdot \mathbf{B})\Omega(\mathbf{k})] \tag{12}$$

Here the prefactor $D(\mathbf{B}, \Omega_{\mathbf{k}}) = (1 + \frac{e}{\hbar}(\mathbf{B} \cdot \Omega(\mathbf{k})))^{-1}$, modifying the invariant phase space volume according to $dkdx \rightarrow D(\mathbf{B}, \Omega_{\mathbf{k}})dkdx$, gives rise to a noncommutative mechanical model, because the Poisson brackets of co-ordinates is nonzero[48]. For ease of notation we will simply denote $D(\mathbf{B}, \Omega_{\mathbf{k}})$ by D for rest of the paper.

The second term of the Eq. (11) gives rise to the anomalous transport induced by the Berry curvature. The third term in the same equation gives rise to chiral magnetic effect modified by the orbital magnetic moment. The chiral magnetic effect, an interesting signature of transport phenomena in Weyl semimetals, appears in equilibrium i.e. $\mathbf{E} = 0$[49–52]. This term implies an electric current $\propto \mathbf{B}$ to flow along the direction of the magnetic field in Weyl semimetals without any electric field in the presence of finite chiral chemical potential $(\mu_+ - \mu_-)$ where μ_+ and μ_- are the chemical potentials of two Weyl nodes[53]. There has been some controversy regarding the existence of the equilibrium chiral magnetic effect in condensed matter systems because the effect described above violates the Maxwell's equations[51,54–56]. It has been discussed that in the dc limit i.e. when frequency is set to zero first, the system is in equilibrium and the chiral magnetic effect vanishes[51]. The second term in Eq. (12) implies the usual Lorentz force modified by $m(\mathbf{k})$ whereas the last term proportional to $\mathbf{E} \cdot \mathbf{B}$ in Eq. (12) is the semi-classical manifestation of the topological effect known as chiral anomaly in the context of topological semimetals. The chiral anomaly in topological Weyl semimetals implies the non-conservation of a chiral current i.e. violation of the separate number conservation law of Weyl Fermions of a given chirality in the presence of parallel electric and magnetic fields. It is important to note that chiral anomaly is a purely quantum mechanical effect, and while the third term in Eq. (12) has been interpreted in the literature as the semi-classical manifestation of chiral anomaly in topological semimetals, the term itself may be non-zero in the presence of non-trivial Berry curvature even in systems that do not support chiral anomaly in the quantum limit.

To calculate planar Hall conductivity, we apply an electric field ($\mathbf{E}$) along the $x-$ axis and a magnetic field ($\mathbf{B}$) in the $x-y$ plane at a finite angle θ from the $x-$ axis, i.e. $\mathbf{B} = B\cos\theta\,\hat{x} + B\sin\theta\,\hat{y}$, $\mathbf{E} = E\hat{x}$. Here, θ is the angle between $\mathbf{E}$ and $\mathbf{B}$ as shown in Fig. 2. After substituting $\dot{\mathbf{r}}$ and $\dot{\mathbf{k}}$ into the Boltzmann equation Eq. (7), it then takes the form,

$$D\Bigg[\left(\frac{eE\tilde{v}_x}{\hbar} + \frac{e^2}{\hbar}BE\,cos\theta(\tilde{\mathbf{v}}_{\mathbf{k}} \cdot \Omega(\mathbf{k}))\right)\frac{\partial\tilde{f}_{eq}}{\partial\tilde{\varepsilon}} + \frac{eB}{\hbar^2}\Bigg(-\tilde{v}_z\,sin\theta\frac{\partial}{\partial k_x} + (\tilde{v}_x\,sin\theta - \tilde{v}_y\,cos\theta)\frac{\partial}{\partial k_z} + \tilde{v}_z\,cos\theta\frac{\partial}{\partial k_y}\Bigg)\tilde{f}_{\mathbf{k}}\Bigg] = -\frac{\tilde{f}_{eq} - \tilde{f}_{\mathbf{k}}}{\tau} \tag{13}$$

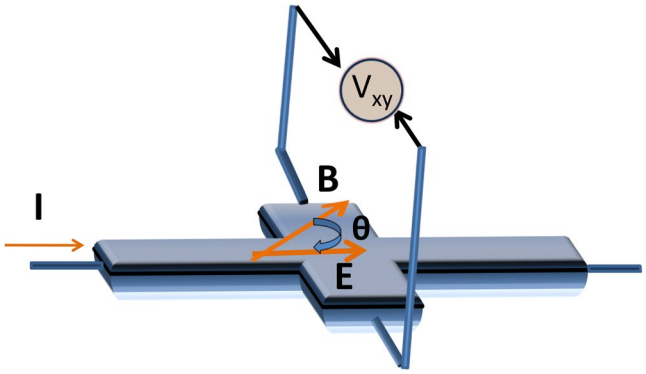

Figure 2. Illustration for the planar Hall effect measurement geometry. The electric field (**E**) is applied along the $x-$ axis and a magnetic field (**B**) in the $x-y$ plane makes a finite angle θ with the **E**. The planar Hall effect is measured as an in-plane voltage (V_{xy}) transverse to the direction of current in the $x-y$ plane.

where $\widetilde{f}_{eq}$ is equilibrium Fermi-Dirac distribution with the energy dispersion $\varepsilon_{\mathbf{k}} = \varepsilon_{0,\mathbf{k}} - \mathbf{m}\cdot\mathbf{B}$ modified due to the orbital magnetic moment.

Keeping only linear order dependence on the applied field **E** and **B**, we now assume following ansatz for the distribution function, $\widetilde{f}_{\mathbf{k}}$, which is a solution to the steady-state Boltzmann equation Eq. (7), can be written as

$$\widetilde{f}_{\mathbf{k}} = \widetilde{f}_{eq} + eDE\tau(\tilde{v}_x + \frac{eB\cos\theta}{\hbar}(\tilde{\mathbf{v}}_{\mathbf{k}}\cdot\mathbf{\Omega}(\mathbf{k})))(\partial_{\tilde{\varepsilon}}\widetilde{f}_{eq}) \tag{14}$$

Now, in the absence of any thermal gradient, we write the charge density (ρ) and current density (J) as[47],

$$\rho = -e\int[d\mathbf{k}]D^{-1}\widetilde{f}_{\mathbf{k}} \tag{15}$$

$$\mathbf{J} = -e\int[d\mathbf{k}](D^{-1}\dot{\mathbf{r}} + \nabla_{\mathbf{r}}\times m_{\mathbf{k}})\widetilde{f}_{\mathbf{k}} \tag{16}$$

where $[d\mathbf{k}] = \frac{d^3\mathbf{k}}{(2\pi)^3}$ and the factor D arises from a field-induced change in the volume of the phase space. The second term of Eq. (16) is a contribution of magnetization current. As we are working with spatially uniform fields, in the present work the expression for the current density takes the following form,

$$\mathbf{J} = -e\int[d\mathbf{k}][\tilde{\mathbf{v}}_{\mathbf{k}} + \frac{e}{\hbar}(\mathbf{E}\times\Omega(\mathbf{k})) + \frac{e}{\hbar}(\tilde{\mathbf{v}}_{\mathbf{k}}\cdot\Omega(\mathbf{k}))\mathbf{B}]\widetilde{f}_{\mathbf{k}} \tag{17}$$

Plugging $\widetilde{f}_k$ into the above equation and comparing it with Eq. (4), we now arrive at the semiclassical formula for the longitudinal electrical conductivity including the effects due to Berry curvature and orbital magnetic moment,

$$\sigma_{xx} = e^2\int\frac{d^3k}{(2\pi)^3}\tau\left[D(\tilde{v}_x + \frac{eB\cos\theta}{\hbar}(\tilde{\mathbf{v}}_{\mathbf{k}}\cdot\Omega(\mathbf{k})))^2\right](-\partial_{\tilde{\varepsilon}}\widetilde{f}_{eq}) \tag{18}$$

In the above equation the anomalous velocity factor $\frac{eB\cos\theta}{\hbar}(\tilde{\mathbf{v}}_{\mathbf{k}}\cdot\Omega(\mathbf{k}))$ appears due to the topological term $(\mathbf{E}\cdot\mathbf{B})$ and the orbital magnetic moment. This term is the origin of finite B-dependent longitudinal electrical conductivity which is independent of **B** for a regular Fermi liquid. When $\theta = 0$, we recover the formula for LEC for parallel **E** and **B** fields as derived in earlier works[53,57–59].

Now we will derive the expression of PHC. Inserting $\widetilde{f}_k$ in Eq. (17) and comparing it with Eq. (4), we write the following expression for the planar Hall conductivity,

$$\begin{aligned}\sigma_{yx}^{\mathrm{ph}} &= e^2\int\frac{d^3k}{(2\pi)^3}D\tau(-\partial_{\tilde{\varepsilon}}\widetilde{f}_{eq})\Big[\tilde{v}_x\tilde{v}_y + \tilde{v}_x\frac{eB\sin\theta}{\hbar}(\tilde{\mathbf{v}}_{\mathbf{k}}\cdot\mathbf{\Omega}(\mathbf{k}))\\ &\quad + \tilde{v}_y\frac{eB\cos\theta}{\hbar}(\tilde{\mathbf{v}}_{\mathbf{k}}\cdot\Omega(\mathbf{k})) + \frac{e^2B^2\sin 2\theta}{2\hbar^2}(\tilde{\mathbf{v}}_{\mathbf{k}}\cdot\Omega(\mathbf{k}))^2\Big]\end{aligned} \tag{19}$$

Here we have neglected terms in the solution which are orders of magnitude smaller than the right hand side of Eq. (19)[32]. It is clear from Eq. (19) that in the absence of Berry curvature and the orbital magnetic moment (i.e. in the absence of magnetic field) the Berry curvature ($\Omega(\mathbf{k})$) dependent terms vanish and $\tilde{v}_x\tilde{v}_y \to v_xv_y$ which is B independent. Since the remaining momentum space integral of Eq. (19) vanishes, the PHC (σ_{xy}^{ph}) identically vanishes in the absence of magnetic field.

Planar Hall conductivity in topological insulators. In this section we show the B-dependence and angular dependence of longitudinal magnetoconductivity and planar Hall conductivity computed using Eqs (18)

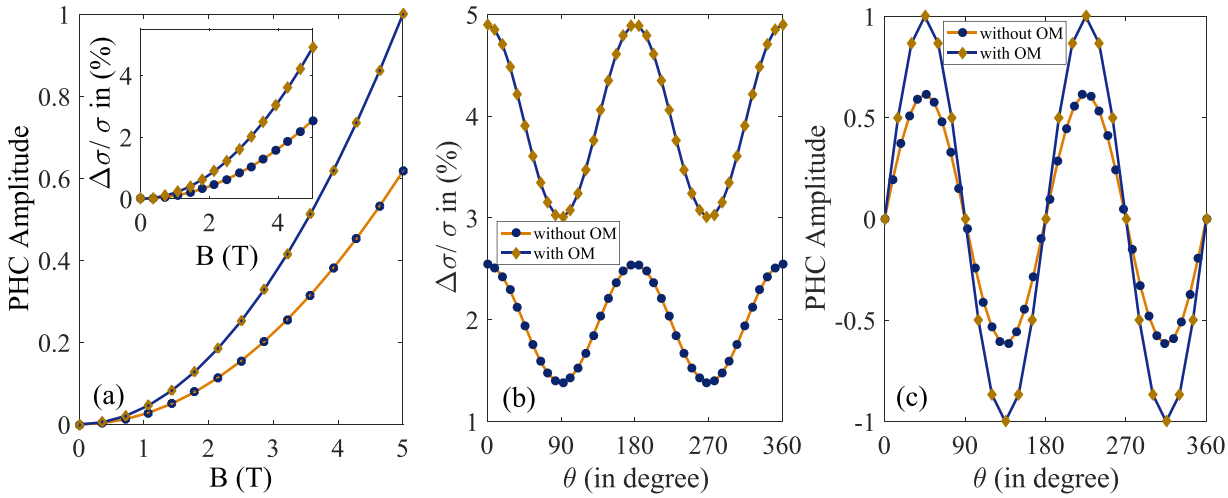

Figure 3. (**a**) Shows the dependence of amplitude of PHC (normalized by the maximum value of PHC in the presence of m) as a function of in-plane magnetic field at $\theta = \pi/4$ and temperature $T = 24$ K. (Inset depicts the LMC in the presence as well as absence of orbital magnetic moment (m) as a function of in-plane magnetic field at $\theta = 0°$. The other parameters are same as above). (**b**,**c**) Show the angular dependence of LMC and PHC (normalized) at $T = 24$ K in the presence and absence of m for $B = 5$ T. Here we have normalized the y axis of (**c**) by the value of PHC at $\theta = \pi/4$ in the presence of m. Curves in yellow indicate the presence of m whereas blue lines are for $m = 0$. In all cases we consider the Fermi level situated at 27 meV from the bottom of the lowest conduction band.

and (19). Negative longitudinal magnetoresistance has recently been observed in several topological insulators in the presence of bulk conduction[8–12]. Although the planar Hall conductivity has recently been observed from the surface states of a 3D topological insulator[38], it is not observed from bulk states till date. In the present work we consider only bulk states and neglect the contribution to conductivity from the surface states.

In the inset of Fig. 3(a) we have plotted the LMC as a function of the applied magnetic field at $T = 24$ K in the presence and absence of m where we have defined LMC as

$$\frac{\Delta\sigma}{\sigma} = \frac{\sigma_{xx}(B) - \sigma_{xx}(B=0)}{\sigma_{xx}(B=0)} \tag{20}$$

The LMC increases monotonically with the magnetic field in both cases and follows the B^2-dependence. The orbital moment, first-order correction to the classical equations of motion, increases the Zeeman splitting between two conduction bands and enhances the LMC significantly. Therefore it is essential to take into account the effect of m in computing magnetoconductivity for topological insulators. Our results indicates the remarkable fact that the non trivial Berry curvature and orbital magnetic moment can produce an anisotropy in the magneto-conductivity even without the chiral anomaly effect. The LMC also follows $\cos^2\theta$ dependence at $B = 5$ T in both cases (presence and absence of m) as depicted in Fig. 3(b), leading to the anisotropic magnetoresistance (AMR).

In Fig. 3(a and c) we have shown the amplitude and angular dependence of planar Hall conductivity in for the bulk states conduction in Bi_2Se_3. The amplitude of the PHC is finite at all field directions except at $\theta = 0$ and $\theta = \pi/2$ and follows a quadratic dependence on B which is similar to what has been observed in experiments on PHC on the surface states of Bi_2Se_3. The amplitude is enhanced significantly due to the presence of m leading to the fact that orbital moment plays a very important role in PHC. The planar Hall conductivity σ_{xy}^{ph} does not satisfy the familiar anti-symmetry relation ($\sigma_{xy} = -\sigma_{yx}$) in the spatial indices and this property can be used to identify PHC in experiments. Within the regime of applicability of quasi-classical formalism, we have found that the PHC follows $\cos\theta \sin\theta$ dependence for $B = 5$ T as depicted in Fig. 3(c). This is also similar what has been observed in experiments on PHC due to surface states of Bi_2Se_3[38].

In the presence of orbital magnetic moment, the LMC and PHC as a function of Fermi energy (E_F) for $B = 5$ T and $T = 24$ K are shown in Fig. 4(a). In experiment, the Fermi level can be tuned by gate voltage. It is clear from the figure that the LMC is enhanced as the Fermi level approaches the band bottom whereas the amplitude of PHC decreases. The temperature dependence of the LMC and PHC at $B = 5$ T in the presence of orbital magnetic moment is depicted in Fig. 4(b). It is clear from the figure that both LMC and PHC decrease with increasing temperature.

Conclusions

In this work we present a quasiclassical theory of planar Hall conductivity due to bulk conduction in 3D strong topological insulators such as Bi_2Se_3 using the phenomenological Boltzmann transport theory. In the presence of bulk conduction, negative longitudinal magnetoresistance has recently been found in these systems[8–12]. Negative longitudinal magnetoresistance in topological semimetals such as Dirac and Weyl semimetals is typically associated with chiral or Adler-Bell-Jackiw anomaly[13–22]. It has recently been shown that this effect can occur also in 3D topological insulators in the presence of bulk conduction even in the absence of chiral anomaly[30]. In this paper we

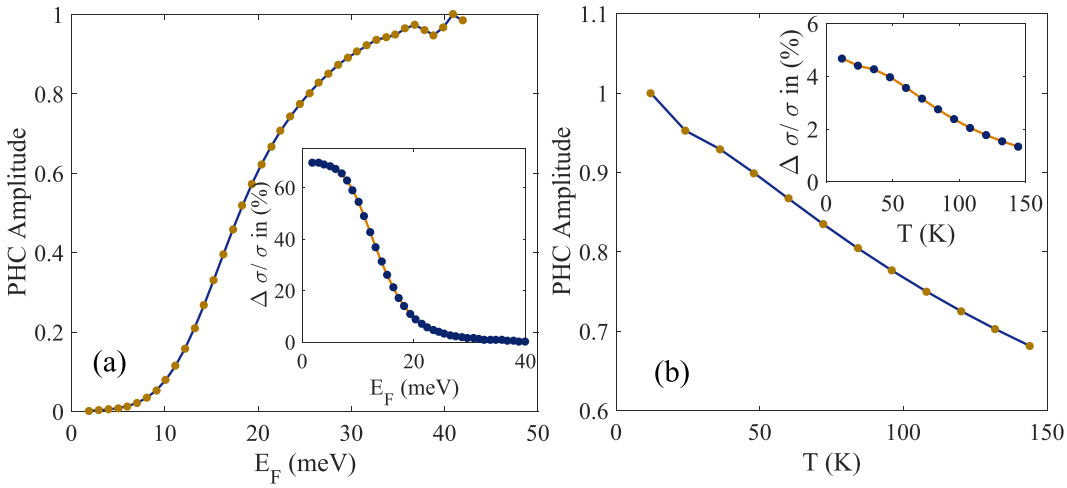

Figure 4. (**a**) Shows the amplitude of planar Hall conductivity ($\theta = \frac{\pi}{4}$) in the presence of orbital magnetic moment as a function of Fermi energy for $B = 5$ T and $T = 24$ K for the bulk states of Bi_2Se_3 (Inset Shows the behavior of LMC ($\theta = 0$) as a function of Fermi energy). It is important to note that the magnitudes of LMC and PHC behave very differently as the band filling approaches the bottom of the conduction bands. The Fermi energy is measured from the bottom of the lowest conduction band. (**b**) Shows the temperature dependence of the amplitude of planar Hall conductivity ($\theta = \frac{\pi}{4}$) in the presence of m for $B = 5$ T for the bulk states of Bi_2Se_3 (Inset shows the temperature dependence of LMC ($\theta = 0$)). The amplitude of PHC has been normalized by its maximum value in both figures.

predict that TI systems supporting negative LMR in the presence of bulk conduction will also exhibit planar Hall effect when the electric and magnetic fields are not perfectly aligned with each other. Note that, a similar effect has recently been predicted also in Weyl semimetals from effects associated with chiral anomaly[31,32]. In the present work we show that such an effect exists also in 3D topological insulators due to Berry curvature of the conduction band even in the absence of chiral anomaly.

In the presence of in-plane electric and magnetic fields not perfectly aligned with each other, we find the non-zero planar Hall response in 3D strong TIs which is very different in nature from the usual Lorentz force mediated Hall response and even the Berry phase mediated anomalous Hall response, both of which are anti-symmetric in spatial indices. We find that both longitudinal magnetoconductivity and planar Hall conductivity follow a quadratic dependence on B. Moreover, for a specific value of the magnetic field, the LMC follows $\cos^2\theta$ dependence whereas the PHC goes as $B^2\cos\theta\sin\theta$, where θ is the angle between the applied **E** and **B** fields. Since in PHC, $\sigma_{yx} \sim \cos\theta\sin\theta$ where **B** makes an angle θ with the electric field **E**, which is taken parallel to the x axis, it follows that PHC is symmetric in the spatial indices, $\sigma_{yx} = \sigma_{xy}$. We find that, in the definition for LMC, Eq. (20), the numerator increases with increasing Fermi Energy E_F, but the rate of increase of the Drude conductivity in the denominator is larger. Consequently LMC has defined in Eq. (20), decreases with E_F while PHC increases with E_F (Fig. 4a). We have derived an analytical expression for planar Hall conductivity taking into account the orbital magnetic moment along with the non trivial Berry curvature of the conduction band. It is clear from our results that orbital magnetic moment enhances the magnitude of both LMC and PHC and is important for their theoretical description. Our numerical results predict experimental observations of PHC together with LMC from the bulk states of 3D strong topological insulators which can be tested in experiments.

References

1. Hasan, M. Z. & Kane, C. L. Colloquium: Topological insulators. *Rev. Mod. Phys.* **82**, 3045–3067 (2010).
2. Qi, X.-L. & Zhang, S.-C. Topological insulators and superconductors. *Rev. Mod. Phys.* **83**, 1057–1110 (2011).
3. Peng, H. *et al.* Aharonov-bohm interference in topological insulator nanoribbons. *Nature Materials* **9**, 225 EP – (2009).
4. Chen, J. *et al.* Gate-voltage control of chemical potential and weak antilocalization in bi_2se_3. *Phys. Rev. Lett.* **105**, 176602 (2010).
5. He, H.-T. *et al.* Impurity effect on weak antilocalization in the topological insulator bi_2se_3. *Phys. Rev. Lett.* **106**, 166805 (2011).
6. Checkelsky, J. G., Hor, Y. S., Cava, R. J. & Ong, N. P. Bulk band gap and surface state conduction observed in voltage-tuned crystals of the topological insulator bi_2se_3. *Phys. Rev. Lett.* **106**, 196801 (2011).
7. Qu, D.-X., Hor, Y. S., Xiong, J., Cava, R. J. & Ong, N. P. Quantum oscillations and hall anomaly of surface states in the topological insulator bi2te3. *Science* **329**, 821–824 (2010).
8. Wiedmann, S. *et al.* Anisotropic and strong negative magnetoresistance in the three-dimensional topological insulator bi_2se_3. *Phys. Rev. B* **94**, 081302 (2016).
9. Wang, L.-X. *et al.* Zeeman effect on surface electron transport in topological insulator bi_2se_3 nanoribbons. *Nanoscale* **7**, 16687–16694 (2015).
10. Wang, J. *et al.* Anomalous anisotropic magnetoresistance in topological insulator films. *Nano Research* **5**, 739–746 (2012).
11. He, H. T. *et al.* Disorder-induced linear magnetoresistance in (221) topological insulator bi_2se_3 films. *Applied Physics Letters* **103**, 031606 (2013).
12. Taskin, A. A., Sasaki, S., Segawa, K. & Ando, Y. Manifestation of topological protection in transport properties of epitaxial bi_2se_3 thin films. *Phys. Rev. Lett.* **109**, 066803 (2012).
13. Goswami, P., Sharma, G. & Tewari, S. Optical activity as a test for dynamic chiral magnetic effect of weyl semimetals. *Phys. Rev. B* **92**, 161110 (2015).

14. Zhong, S., Orenstein, J. & Moore, J. E. Optical gyrotropy from axion electrodynamics in momentum space. *Phys. Rev. Lett.* **115**, 117403 (2015).
15. Goswami, P. & Tewari, S. Axionic field theory of (3 + 1)-dimensional weyl semimetals. *Phys. Rev. B* **88**, 245107 (2013).
16. Adler, S. L. Axial-vector vertex in spinor electrodynamics. *Phys. Rev.* **177**, 2426–2438 (1969).
17. Nielsen, H. & Ninomiya, M. A no-go theorem for regularizing chiral fermions. *Physics Letters B* **105**, 219–223 (1981).
18. Nielsen, H. & Ninomiya, M. The adler-bell-jackiw anomaly and weyl fermions in a crystal. *Physics Letters B* **130**, 389–396 (1983).
19. Aji, V. Adler-bell-jackiw anomaly in weyl semimetals: Application to pyrochlore iridates. *Phys. Rev. B* **85**, 241101 (2012).
20. Zyuzin, A. A., Wu, S. & Burkov, A. A. Weyl semimetal with broken time reversal and inversion symmetries. *Phys. Rev. B* **85**, 165110 (2012).
21. Xu, G., Weng, H., Wang, Z., Dai, X. & Fang, Z. Chern semimetal and the quantized anomalous hall effect in $hgcr_2se_4$. *Phys. Rev. Lett.* **107**, 186806 (2011).
22. Wan, X., Turner, A. M., Vishwanath, A. & Savrasov, S. Y. Topological semimetal and fermi-arc surface states in the electronic structure of pyrochlore iridates. *Phys. Rev. B* **83**, 205101 (2011).
23. Bell, J. S. & Jackiw, R. A pcac puzzle: $\pi^0 \to \gamma\gamma$ in the σ-model. *Il Nuovo Cimento A (1965-1970)* **60**, 47–61 (1969).
24. He, L. P. *et al*. Quantum transport evidence for the three-dimensional dirac semimetal phase in cd_3as_2. *Phys. Rev. Lett.* **113**, 246402 (2014).
25. Liang, T. *et al*. Ultrahigh mobility and giant magnetoresistance in the dirac semimetal?cd_3as_2. *Nature Materials* **14**, 280 EP – (2014).
26. Zhang, C.-L. *et al*. Signatures of the adler-bell-jackiw chiral anomaly in a weyl fermion semimetal. *Nature Communications* **7**, 10735 EP – (2016).
27. Li, Q. *et al*. Chiral magnetic effect in zrte5. *Nature Physics* **12**, 550 EP – (2016).
28. Hirschberger, M. *et al*. The chiral anomaly and thermopower of weyl fermions in the half-heusler?gdptbi. *Nature Materials* **15**, 1161 EP – (2016).
29. Xiong, J. *et al*. Evidence for the chiral anomaly in the dirac semimetal na3bi. *Science* **350**, 413 (2015).
30. Dai, X., Du, Z. Z. & Lu, H.-Z. Negative magnetoresistance without chiral anomaly in topological insulators. *Phys. Rev. Lett.* **119**, 166601 (2017).
31. Burkov, A. A. Giant planar hall effect in topological metals. *Phys. Rev. B* **96**, 041110 (2017).
32. Nandy, S., Sharma, G., Taraphder, A. & Tewari, S. Chiral anomaly as the origin of the planar hall effect in weyl semimetals. *Phys. Rev. Lett.* **119**, 176804 (2017).
33. Dinh, K. V. Planar hall effect in ferromagnetic films. *physica status solidi (b)* **26**, 565–569 (1968).
34. Bowen, M., Friedland, K.-J., Herfort, J., Schönherr, H.-P. & Ploog, K. H. Order-driven contribution to the planar hall effect in fe_3Si thin films. *Phys. Rev. B* **71**, 172401 (2005).
35. Goennenwein, S. T. B. *et al*. Planar hall effect and magnetic anisotropy in epitaxially strained chromium dioxide thin films. *Applied Physics Letters* **90**, 142509 (2007).
36. Friedland, K.-J., Bowen, M., Herfort, J., Schönherr, H. P. & Ploog, H. K. Intrinsic contributions to the planar hall effect in fe and fe 3 si films on gaas substrates. *Journal of Physics: Condensed Matter* **18**, 2641 (2006).
37. Ge, Z. *et al*. Magnetization reversal in (Ga, Ma)As/MnO exchange-biased structures: Investigation by planar hall effect. *Phys. Rev. B* **75**, 014407 (2007).
38. Taskin, A. A. *et al*. Planar hall effect from the surface of topological insulators. *Nature Communications* **8**, 1340 (2017).
39. Xia, Y. *et al*. Observation of a large-gap topological-insulator class with a single dirac cone on the surface. *Nature Physics* **5**, 398 EP – (2009).
40. Zhang, H. *et al*. Topological insulators in bi_2se_3, bi_2te_3 and sb_2te_3 with a single dirac cone on the surface. *Nature Physics* **5**, 438 EP (2009).
41. Nechaev, I. A. & Krasovskii, E. E. Relativistic $k \cdot p$ hamiltonians for centrosymmetric topological insulators from ab initio wave functions. *Phys. Rev. B* **94**, 201410 (2016).
42. Shun-Qing, S. *Topological insulators*. (Springer-Verlag, Berlin Heidelberg, 2012).
43. Xiao, D., Chang, M.-C. & Niu, Q. Berry phase effects on electronic properties. *Rev. Mod. Phys.* **82**, 1959–2007 (2010).
44. M. Ziman, J. *Electrons and phonons: the theory of transport phenomena in solids*. (Oxford, UK: Clarendon Press, 2001).
45. Burkov, A. A. Chiral anomaly and diffusive magnetotransport in weyl metals. *Phys. Rev. Lett.* **113**, 247203 (2014).
46. Sundaram, G. & Niu, Q. Wave-packet dynamics in slowly perturbed crystals: Gradient corrections and berry-phase effects. *Phys. Rev. B* **59**, 14915–14925 (1999).
47. Morimoto, T., Zhong, S., Orenstein, J. & Moore, J. E. Semiclassical theory of nonlinear magneto-optical responses with applications to topological dirac/weyl semimetals. *Phys. Rev. B* **94**, 245121 (2016).
48. Duval, C., Horváth, Z., Horváthy, P. A., Martina, L. & Stichel, P. C. Berry phase correction to electron density in solids and "exotic" dynamics. *Modern Physics Letters B* **20**, 373–378 (2006).
49. Son, D. T. & Yamamoto, N. Berry curvature, triangle anomalies, and the chiral magnetic effect in fermi liquids. *Phys. Rev. Lett.* **109**, 181602 (2012).
50. Stephanov, M. A. & Yin, Y. Chiral kinetic theory. *Phys. Rev. Lett.* **109**, 162001 (2012).
51. Chen, Y., Wu, S. & Burkov, A. A. Axion response in weyl semimetals. *Phys. Rev. B* **88**, 125105 (2013).
52. Fukushima, K., Kharzeev, D. E. & Warringa, H. J. Chiral magnetic effect. *Phys. Rev. D* **78**, 074033 (2008).
53. Kim, K.-S., Kim, H.-J. & Sasaki, M. Boltzmann equation approach to anomalous transport in a weyl metal. *Phys. Rev. B* **89**, 195137 (2014).
54. Vazifeh, M. M. & Franz, M. Electromagnetic response of weyl semimetals. *Phys. Rev. Lett.* **111**, 027201 (2013).
55. Başar, G. M. C., Kharzeev, D. E. & Yee, H.-U. Triangle anomaly in weyl semimetals. *Phys. Rev. B* **89**, 035142 (2014).
56. Landsteiner, K. Anomalous transport of weyl fermions in weyl semimetals. *Phys. Rev. B* **89**, 075124 (2014).
57. Son, D. T. & Spivak, B. Z. Chiral anomaly and classical negative magnetoresistance of weyl metals. *Phys. Rev. B* **88**, 104412 (2013).
58. Lundgren, R., Laurell, P. & Fiete, G. A. Thermoelectric properties of weyl and dirac semimetals. *Phys. Rev. B* **90**, 165115 (2014).
59. Sharma, G., Goswami, P. & Tewari, S. Nernst and magnetothermal conductivity in a lattice model of weyl fermions. *Phys. Rev. B* **93**, 035116 (2016).
60. Wolos, A. *et al*. *g*-factors of conduction electrons and holes in Bi_2Se_3 three-dimensional topological insulator. *Phys. Rev. B* **93**, 155114 (2016).

Acknowledgements

SN acknowledges MHRD, India for research fellowship.

Author Contributions

S.T. conceived the problem. S.N. performed the calculations. S.N., A.T. and S.T. analysed the results. S.N., A.T. and S.T. wrote the paper. All authors reviewed the manuscript.

Additional Information

Competing Interests: The authors declare no competing interests.